

# A model for multifragmentation in heavy-ion reactions

A. Ferrari<sup>1</sup>, M.V. Garzelli<sup>2,3\*</sup>, P.R. Sala<sup>2</sup>

<sup>1</sup>CERN, Geneva, Switzerland

<sup>2</sup>INFN & Università di Milano, Dipartimento di Fisica, Milano, Italy

<sup>3</sup>Universidad de Granada, Departamento de Física Teórica y del Cosmos, Granada, Spain

## Abstract

From an experimental point of view, clear signatures of multifragmentation have been detected by different experiments. On the other hand, from a theoretical point of view, many different models, built on the basis of totally different and often even contrasting assumptions, have been provided to explain them. In this contribution we show the capabilities and the shortcomings of one of this models, a QMD code developed by us and coupled to the nuclear de-excitation module taken from the multipurpose transport and interaction code FLUKA, in reproducing the multifragmentation observations recently reported by the INDRA collaboration for the reaction Nb + Mg at a 30 MeV/A projectile bombarding energy. As far as fragment production is concerned, we also briefly discuss the isoscaling technique by considering reactions characterized by a different isospin asymmetry, and we explain how the QMD + FLUKA model can be applied to obtain information on the slope of isotopic yield ratios, which is crucially related to the symmetry energy of asymmetric nuclear matter.

## 1 Features of multifragmentation

When studying heavy-ion collisions at non-relativistic energies, multifragmentation can be observed for the most central ones, in a range of projectile-ion bombarding energies from tens MeV/A up to a few hundreds MeV/A, depending of the properties of the nuclei under consideration. Many issues of this phenomenon are still under discussion, in particular concerning the stage at which it occurs in the evolution of a reaction, e.g. if a nuclear system undergoing multifragmentation is or not equilibrated, how a simultaneous break-up in multiple fragments can occur, and if the multifragmentation is the result of a phase-transition.

According to the currently most believable scenario, during the overlapping stage of heavy-ion collisions (typical time  $\simeq 100$  fm/c) matter can undergo compression, leading to large excitation energies. As a consequence, the blob of nuclear matter starts to expand and can go on expanding down to sub-saturation densities ( $\rho \simeq 0.1 - 0.3 \rho_0$ , where  $\rho_0$  is the normal nuclear matter density) and reach temperatures  $\simeq 3 - 8$  MeV, where it becomes unstable and breaks up into multiple fragments. These conditions are typical of a liquid-gas coexistence region [1, 2].

As already mentioned, one of the open issues is if equilibration is reached in these reactions. A statistical description of multifragmentation is based on this assumption. A dynamical description of multifragmentation instead is not based on this assumption. Difficulties in coming to a non-controversial conclusion are largely due to the fact that most of the experimental data refer to patterns of particles detected just in the last stage of the reactions, involving channels fed by the sequential decays which heavily affect and modify the primary fragment distribution.

Multifragmentation can be distinguished from other decay channels on the basis of the excitation energy: a typical scenario of small excitation energies ( $E < 2 - 3$  MeV/A) is characterized by the

---

\*Corresponding author e-mail: [Maria.Garzelli@mi.infn.it](mailto:Maria.Garzelli@mi.infn.it) Proceedings of a talk presented at the 12<sup>th</sup> International Conference on Nuclear Reaction Mechanisms, Varenna, Italy, June 15 - 19 2009

formation of a compound-like system and by its evolution through binary sequential decays (evaporation/fission), whereas for high excitation energies ( $E > 3 \text{ MeV/A}$ ) multifragmentation in a finite volume and a simultaneous break-up into multiple fragments can occur. The excitation energy is indeed related to the mass asymmetry ( $A_{proj} - A_{target}$ ): in case of symmetric central reactions the compression is responsible of the high excitation energy, whereas in case of asymmetric reactions only a partial compression can occur and a large part of the excitation energy appears in the form of thermal energy [3]. In all cases, multifragmentation is typically driven by the following expansion.

Due to its mentioned features, multifragmentation, occurring during the phase of expansion of the nuclear system formed by an ion-ion (central) collision, allows to study the nuclear Equation of State (EoS) at subnormal nuclear densities. In particular, it is possible to infer useful information concerning the symmetry energy and its density dependence, by investigating the isotopic yield distributions of the emitted fragments. The isoscaling technique, based on the analysis of isotopic yield ratios obtained in reactions with a different isospin asymmetry, has been developed with this purpose.

After an overview of the models to study multifragmentation in Section 2, and a brief presentation of the one used in this work in Subsection 2.1, examples of its application in the isoscaling technique and in the reconstruction of multifragmenting sources at energies of a few tens MeV/A are provided in Subsection 3.1 and 3.2, respectively. Finally, our perspectives on further applications of our model are drawn in Section 4.

## 2 Models to study multifragmentation

One can distinguish between

- Dynamical Models: some of them are 1-body approaches, inspired to the BUU/BNV/Landau-Vlasov transport theory. Alternatively, n-body approaches have been developed, such as the QMD/AMD/FMD. n-body approaches are very powerful in the description of the simultaneous break-up of a nuclear system in multiple fragments, since they preserve correlations among nucleons.
- Statistical Models: they assume to work with an equilibrated excited source at freeze-out (thermal equilibrium). Taking into account that the nuclear system undergoes an expansion, leading to decreasing densities, down to subnormal values, the freeze-out [4] occurs when the mutual nuclear interaction among fragments can be neglected. Statistical models have been worked out both in the grand-canonical framework (see e.g. Ref. [5]) and in the micro-canonical framework. The most widespread among the last ones is the SMM [1, 6, 7] and its modifications ISMM [8] and SMM-TF [9].

We emphasize that the onset of multifragmentation according to dynamical models is different from the description of multifragmentation according to statistical models. In fact, in the statistical models a source in thermal equilibrium is assumed to fragment. This means that memory effects concerning how the source has been originated are neglected. On the other hand, in the dynamical models multifragmentation is a fast process: the involved nucleons have not the time to come to equilibrium. Fragments originate from the density fluctuations (nucleon-nucleon correlations) due to collisions in the ion-ion overlapping stage, which survive the expansion phase (memory effects). The chemical composition of hot fragments is expected to play a role in helping to disentangle the nature (dynamical / statistical) of the multifragmentation mechanism [10].

Different models reproduce different features of the collisions with different success. A mixed model, inspired to the QMD dynamical approach to describe the fast stage of ion-ion collisions and to a statistical approach to describe the further decay of the multiple primary excited fragments produced by QMD down to their ground state, has been used to obtain the results presented in this work. Due to the crucial role of dynamics, as supported by our results, in the following we mainly concentrate on the description of the dynamical aspects of multifragmentation.

## 2.1 QMD/AMD approaches

In these microscopic models a nucleus is considered a set of mutually interacting nucleons. The propagation of each nucleon occurs according to a classical Hamiltonian with quantum effects [11]. In particular, nucleons are described by gaussian wave packets. Each of them moves under the effects of a potential given by the sum of the contribution of all other nucleons (2-body effects). Furthermore, when two nucleons come very close to each other, they can undergo elastic collisions (nucleon-nucleon stochastic scattering cross-sections) with Pauli blocking.

A proper treatment of antisymmetrization is implemented in AMD [12]. On the other hand, QMDs do not provide any antisymmetrization of the nuclear wave-function. An approximate effect can be obtained through the inclusion in the Hamiltonian of a Pauli potential term, or through the implementation of specific constraints.

Still open questions in molecular dynamics approaches concern the functional form of the nucleon-nucleon potential (each working group who developed a molecular dynamics code has its preferred choice of terms), the potential parameters and their relation to the nuclear matter EoS. Nowadays, many groups prefer parameter sets leading to a soft EoS. Anyway, there are open questions concerning the symmetry term [13, 14]. In particular, a stiff dependence for this term means that the symmetry energy always increases with increasing densities. On the other hand, a soft dependence means that the symmetry energy decreases at high densities. At present, a stiff dependence seems more reliable than a soft one. Many uncertainties come from the fact that our observations are mainly based on symmetric nuclear matter ( $N/Z \simeq 1$ ) near normal nuclear density ( $\simeq 0.16 \text{ fm}^{-3}$ ), since it is difficult to obtain highly asymmetric nuclear matter in terrestrial laboratories. On the other hand these studies are crucial to understand features of astrophysical objects (such as neutron star formation and structure), where conditions of extreme neutron-proton asymmetry can be present.

Other open issues concern the gaussian width, the use of in-medium nucleon-nucleon cross-sections instead of free nucleon-nucleon cross-sections (in QMD the free choice is usually implemented, whereas in the AMD the in-medium choice has been implemented), the question of how long the dynamical simulation has to be carried over and the problem of the development of a fully relativistic approach (on the last point see e.g. Ref. [15]).

A QMD code has been developed by us [16] in fortran 90. It includes a 3-body repulsive potential and a surface term (attractive at long distances and repulsive at short distances). Pauli blocking is implemented by means of the CoMD constraint [17]. Neutron and proton are fully distinguished by means of a symmetry term and an isospin dependent nucleon-nucleon stochastic scattering cross-section. The kinematics is relativistic and attention is paid to the conservation of key quantities (total energy/momentum, etc.) in each ion-ion collision. Simulations are performed by means of our code from the ion-ion overlapping stage up to  $t \simeq 200 - 300 \text{ fm}/c$  (fast stage of the reaction). The description of the de-excitation of the excited fragments present at the end of the fast stage is obtained through the coupling of our QMD with the statistical model taken from the PEANUT module available in the FLUKA Monte Carlo code [18–21] in a version for the g95 compiler. Up to now, the QMD + FLUKA interface has been tested in the collisions of ions with charge up to  $Z=86$  (radon isotopes), providing interesting results (see e.g. Ref. [22] and references therein).

## 3 Results

### 3.1 Isospin dependence in fragment production: application of the isoscaling technique

The isoscaling technique, already mentioned in Section 1, is based on ratio of yields taken in multifragmentation reactions with similar total size, but different isospin asymmetries  $(N - Z) / (N + Z)$  [23, 24]:

$$R_{21}(N, Z) = Y_2(N, Z)/Y_1(N, Z) = \text{Const} \exp(A_{\text{coeff}}N + B_{\text{coeff}}Z). \quad (1)$$

The numerator of this formula refers to the yield of a given fragment ( $N, Z$ ) obtained from a neutron rich nucleus-nucleus reaction system, whereas the denominator refers to the yield of the same fragment from a neutron poor (more symmetric) reaction at the same energy.  $A_{coeff}$  is related to the symmetry energy and is increasingly larger for couple of reactions with increasingly different isospin composition  $N/Z$ .

In particular, we have considered the neutron rich systems Ar + Fe ( $N/Z = 1.18$ ) and Ar + Ni ( $N/Z = 1.13$ ) with respect to the neutron poor system Ca + Ni ( $N/Z = 1.04$ ). Among other authors, these systems have been previously studied by [25] (see also Ref. [26,27]).

Isotopic yield ratios for light fragment ( $Z \leq 8$ ) emission have been obtained from our QMD + FLUKA simulations for the couple of reactions Ar + Ni / Ca + Ni and Ar + Fe / Ca + Ni at 45 MeV/A projectile bombarding energy. When plotted in the logarithmic plane, isotopic yield ratios for each fixed  $Z$  turn out to be approximately linear, with a slope given by a  $A_{coeff}$ , as expected from Eq. (1). As for the isoscaling parameter  $A_{coeff}$ , our simulations give the following insights:

- The results of our analysis are quite sensitive to the number of isotopes included in the linear fit, at fixed  $Z$  (i.e. to the goodness of the gaussian approximation to the fragment isotopic distribution).
- $A_{coeff}$  differs with  $Z$ , in agreement with [23], which claims that isoscaling is observed for a variety of reaction mechanisms, from multifragmentation to evaporation to deep inelastic scattering, with different slopes in the logarithmic plane.
- $A_{coeff}$  is larger for the couple of reactions with larger difference in the isospin compositions ( $N_1/Z_1 - N_2/Z_2$ ).
- Our average values  $A_{coeff} = 0.18$  for Ar + Ni / Ca + Ni and  $A_{coeff} = 0.31$  for Ar + Fe / Ca + Ni are larger than the experimental values [25], but the comparison is not so meaningful, since it is largely affected by the fact that we include fragments emitted in all directions in our preliminary analysis, whereas in the experiment only fragments emitted at  $44^\circ$  were selected.
- $A_{coeff}$  turns out to be affected by the choice of the impact parameter and decreases significantly when selecting only the most central events.
- $A_{coeff,hot}$  at the end of the overlapping stage can be larger than  $A_{coeff}$  at the end of the full simulation by no more than 20%, at least for the reaction systems under study.

As far as the emissions at preequilibrium are concerned, our simulations lead to the following results:

- For central collisions of Ca + Ni the yield of emitted protons turns out to be larger than the yield of emitted neutrons by 20%. For central collisions of Ar + Ni and Ar + Fe, on the other hand, the yield of emitted protons turns out to be lower than the yield of emitted neutrons by 10 - 15%.
- For each of the three systems under study, the fragment asymmetry of the liquid phase  $(Z/A)_{liq}$  at the end of the preequilibrium stage turns out to be lower than the corresponding value at  $t = 0$ , in qualitative agreement with the AMD simulations [25].
- No traces of isospin fractionation appear, expected indeed for systems with an higher  $N/Z$  content (e.g.  $^{60}\text{Ca} + ^{60}\text{Ca}$ ).

The dependence of our results on the projectile bombarding energy is currently under study, by considering the same reactions at different bombarding energies.

### 3.2 Multifragmenting source reconstruction in Nb + Mg reactions at 30 MeV/A

Multifragmentation has been observed in Nb + Mg reactions at a 30 MeV/A projectile bombarding energy in an experiment performed at the INDRA detector by the INDRA + CHIMERA collaborations [28]. Event selection has been performed, according to experimental cuts on the momentum along the beam axis,  $p_{z,det} > 0.6 p_{z,tot}$ , and on the angular acceptance of the INDRA detector,  $4^\circ < \theta < 176^\circ$ . The

selected events have then been assigned to different regions, corresponding to portions of the plane identified by the total transverse energy and the total multiplicity of charged particles detected in each event. Three regions have been singled out this way, as shown in Fig. 2 of Ref. [28]. We have applied the same selection procedure by implementing proper cuts and filters on the simulated events obtained by our QMD + FLUKA. The selected theoretical events are plotted in Fig. 1, which can be directly compared with Fig. 2 of Ref. [28] and turns out to be in good agreement. The events plotted in the T1 region (red) are the less dissipative ones (more peripheral collisions), whereas the events in the T3 region (blue) correspond to more dissipative (central) collisions.

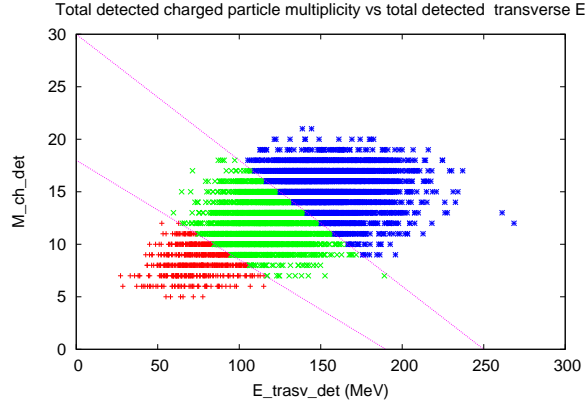


**Fig. 1:** Multifragmentation of Nb + Mg at 30 MeV/A: event selection and identification of different regions T1 (red), T2 (green) and T3 (blue) by our QMD + FLUKA simulations. Each point corresponds to a different ion-ion reaction event in the plane identified by the total multiplicity of detected charged particles and the detected total transverse energy.

For each of the three regions, average values of interesting quantities have been obtained both in the experiment and in the theoretical simulations. Our results, concerning the transverse energy, the multiplicity of charged particles, the velocity and the charge of the biggest residual averaged over all events belonging respectively to the T1, T2 and T3 regions are shown in Table 1. As far as the average transverse energy and multiplicity of charged particle are concerned, the results of our simulations turn out to be in good agreement with the experimental data, within the experimental uncertainties, in the region T1 and T2, corresponding respectively to peripheral and semiperipheral collisions, whereas in case of central collisions the theoretical average transverse energy underestimates the experimental one and the theoretical multiplicity of charged particles slightly overestimates the experimental result. On the other hand, as for the properties of the largest residual, the results of the theoretical simulations show good agreement with experimental data especially for the most central collisions, belonging to the T3 region, whereas for the more peripheral ones the theory overestimates the velocity and the charge of the largest residual. These results, considered all together, seem to point out to the fact that in the experiment the interacting nuclei are slightly more stopped than in the simulation.

Furthermore, the considered experiment aim at the reconstruction of the properties of the so-called source, the blob of matter formed by compression in the ion-ion overlapping stage, which undergoes multifragmentation. Since the experiment detects final cold fragments, i.e. fragments in their ground state after the de-excitation, a procedure has been established to reconstruct the properties of the source by using the observed properties of the final fragments and emitted protons. In particular, the source is isolated by a selection in parallel velocity of different fragments (velocity cuts), by considering different cuts in different regions. The velocity cuts implemented are summarized in Table 2 of Ref. [28]. As far as the proton are concerned, the parallel velocity cut is fixed to 3 cm/ns, whereas for increasingly heavier fragments the velocity cuts are fixed to increasing values. The velocities of the emitted fragments

**Table 1:** Multifragmentation in Nb + Mg at 30 MeV/A: average values of interesting quantities in the regions T1, T2 and T3.

Region	$\langle E_{trasp} \rangle$	$\langle M_{tot} \rangle$	$\langle v_{maxres} \rangle$	$\langle Z_{maxres} \rangle$
Experiment (from Ref. [28]):				
T1	72.9 (10.1)	8.1 (0.8)	6.6 (0.2)	34.1 (2.3)
T2	120.9 (10.6)	11.2 (0.9)	6.4 (0.2)	31.9 (2.7)
T3	176.4 (13.8)	13.4 (1.0)	6.3 (0.2)	30.5 (2.8)
Theoretical simulations (QMD + FLUKA de-exc.):				
T1	74.8	8.4	7.0	38.8
T2	115.8	12.0	6.6	35.7
T3	155.1	15.3	6.2	31.1

are easily obtained even from our simulation by QMD + FLUKA, so it is possible to apply the same procedure for the reconstruction of the source properties even in case of our simulation. As an example, the velocities of the emitted protons obtained by our simulation for events in each of the three regions are shown in Fig. 2, by plotting their perpendicular component  $v_{perp}$  vs. their component along the beam axis  $v_{par}$ . This figure can be compared with Fig.3 of Ref. [28]. The vertical line in each panel corresponds to the  $v_{par}$  cut implemented in the reconstruction of the source.

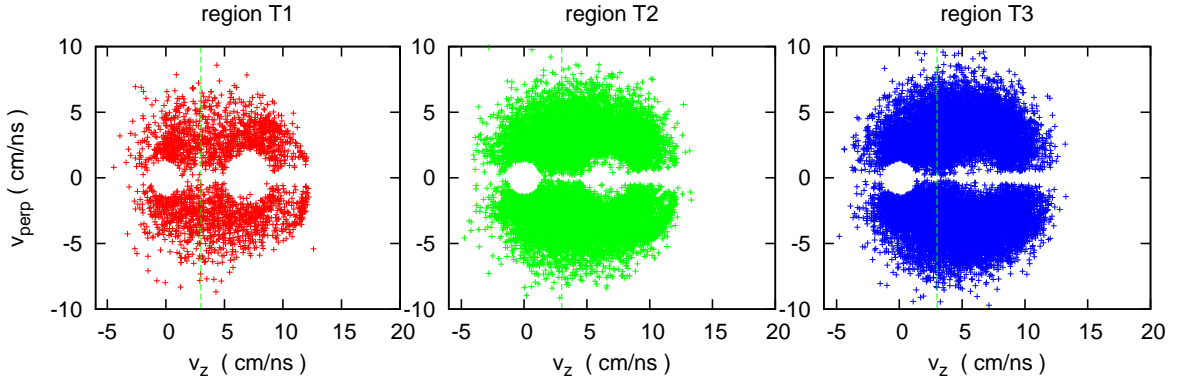


**Fig. 2:** Multifragmentation of Nb + Mg at 30 MeV/A:  $v_{perp}$  vs.  $v_{par}$  for protons emitted in the region T1 (left panel), T2 (central panel) and T3 (right panel), respectively, as obtained by our QMD + FLUKA simulations. Each point in each panel correspond to a different emitted proton. The vertical lines correspond to the velocity cuts implemented for the reconstruction of the multifragmenting sources.

Since the experiment is able to detect the charge of the emitted fragments but not their mass, the velocity cuts can be directly used just to obtain the charge of the source  $Z_s$ . To calculate the mass of the source  $A_s$  a further hypothesis is needed. The author of Ref. [28] assume that the source has the same isotopic ratio as the projectile, i.e.  $A_s/Z_s = A_{proj}/Z_{proj}$ . Source properties in the three regions T1, T2 and T3, as reconstructed both from the experiment and from our simulation, are shown in Table 2. Since the theoretical model allows to simulate even the process of source formation in a straightforward way, the properties of the source can be directly obtained before its de-excitation and break-up into multiple fragments, without using an a-posteriori reconstruction based on velocity cuts. If we identify the source with the biggest fragment present just at the end of the QMD simulation, we obtain a very

good agreement with the experimental results of Ref. [28], especially in the region T1 and T2, even if the experimental results are based on the a-posteriori reconstruction, as can be inferred from Table 2. On the other hand, if we use a reconstruction procedure analogous to the one adopted by the authors of Ref. [28], we overestimate the size of the source, especially for the most central collisions. Finally, as for the average multiplicity of IMF fragments ( $Z \geq 3$ ) subsequently emitted from the source, we obtain good agreement with the experiment in all regions.

**Table 2:** Multifragmentation in Nb + Mg @ 30 MeV/A: reconstruction of the source properties in the regions T1, T2 and T3

Experiment (from Ref. [28]):					
Region	$\langle Z_s \rangle$	$\langle A_s \rangle$	$\langle M_p \rangle$	$\langle M_\alpha \rangle$	$\langle M_{frag} \rangle$
T1	40.7 (2.0)	91.2 (4.7)	2.0 (0.6)	1.1 (0.5)	1.2 (0.4)
T2	42.8 (2.1)	96.0 (4.9)	2.7 (0.7)	1.8 (0.6)	1.4 (0.3)
T3	45.1 (2)	101.3 (4.6)	3.1 (0.7)	2.5 (0.7)	1.6 (0.3)
Theoretical simulation:					
Region	$\langle Z_s \rangle$	$\langle A_s \rangle$	$\langle M_p \rangle$	$\langle M_\alpha \rangle$	$\langle M_{frag} \rangle$
Source properties reconstruction from final secondary fragments (QMD + FLUKA de-exc):					
T1	42.6	96.2	2.2	0.4	1.0
T2	45.1	101.5	3.5	1.6	1.25
T3	48.5	109.5	4.2	3.8	1.5
Source properties at the end of the QMD simulation (primary fragments):					
T1	41.0	91.0			
T2	43.3	96.6			
T3	47.5	106.1			

## 4 Conclusions and perspectives

The QMD model developed in Milano and coupled to the de-excitation module of the Monte Carlo FLUKA code has been used to study reactions between ions of intermediate mass which exhibit multifragmentation features. The results presented in this paper are encouraging, and can be further refined by more precisely investigating up to which extent the statistical de-excitation process from FLUKA modifies the pattern of primary fragments originated dynamically by QMD, and how the results of the simulation change when the time of the transition from the dynamical description of the nuclear system to a statistical description is modified.

Further studies at non relativistic energies that we are going to perform with our theoretical simulation tool concern:

- the isospin distillation effect: it occurs in the multifragmentation of charge-asymmetric systems, and leads to IMF fragments (liquid) more symmetric with respect to the initial matter, and light fragments (gas) more neutron rich. This effect is related to the density dependence of the symmetry energy.
- The bimodality in the probability distribution of the largest fragment as a function of the mass number  $A_{max}$  of the largest fragment, as a signature of a phase transition. Experimental data on this effect have been obtained by the CHIMERA collaboration (see e.g. Ref. [29]).
- (Complete) fusion cross-sections (this kind of analysis has already been performed by other groups, e.g. by means of the ImQMD model [30]).

## Acknowledgements

We wish to thank L. Manduci for enlightening comments on the data on the reaction Nb + Mg at 30 MeV/A collected at the INDRA detector. The QMD code developed by us and used in this study is the fruit of a collaboration involving many people along the years. In particular, we would like to mention F. Ballarini, G. Battistoni, F. Cerutti, A. Fassò, E. Gadioli, A. Ottolenghi, M. Pelliccioni, L.S. Pinsky and J. Ranft for their support and suggestions. The FLUKA code is under continuous development and maintenance by the FLUKA collaboration and is copyrighted by the INFN and CERN.

## References

- [1] J.P. Bondorf *et al.*, *Phys. Rep.* **257** (1995) 133.
- [2] N. Buyukcizmeci *et al.*, *Phys. Rev. C* **77** (2008) 034608 [arXiv:0711.3382 [nucl-th]].
- [3] J. Singh *et al.*, *Phys. Rev. C* **62** (2000) 044617.
- [4] W. Trautmann *et al.*, *Phys. Rev. C* **76** (2007) 064606 [arXiv:0708.4115 [nucl-ex]].
- [5] G. Chauduri, S. Das Gupta, *Phys. Rev. C* **76** (2007) 014619.
- [6] A.S. Botvina *et al.* *Nucl. Phys. A* **475** (1987) 663.
- [7] S. Das Gupta and A.Z. Mekjian, *Phys. Rev. C* **57** (1998) 1361.
- [8] W.P. Tan *et al.*, *Phys. Rev. C* **68** (2003) 034609 [arXiv:nucl-ex/0311001].
- [9] S.R. Souza *et al.*, *Phys. Rev. C* **79** (2009) 054602.
- [10] P.M. Milazzo *et al.*, *Phys. Rev. C* **62** (2000) 041602 [arXiv:nucl-ex/0002012].
- [11] J. Aichelin, *Phys. Rep.* **202** (1991) 233.
- [12] A. Ono and H. Horiuchi, *Phys. Rev. C* **53** (1996) 2958 [arXiv:nucl-th/9601008].
- [13] B.A. Li *et al.*, *Phys. Rep.* **464** (2008) 113.
- [14] V. Baran *et al.*, *Phys. Rep.* **410** (2005) 335 [arXiv:nucl-th/0412060].
- [15] D. Mancusi *et al.*, *Phys. Rev. C* **79** (2009) 014614.
- [16] M.V. Garzelli *et al.*, *Adv. Space Res.* **40** (2007) 1350 [arXiv:nucl-th/0611041].
- [17] M. Papa *et al.*, *Phys. Rev. C* **64** (2001) 024612 [arXiv:nucl-th/0012083].
- [18] G. Battistoni *et al.*, Proc. Hadronic Shower Simulation Workshop, Batavia, Illinois, US, September 6 - 8, 2006, *AIP Conf. Proc.* **896** (2007) 31.
- [19] A. Fassò *et al.*, Proc. CHEP'03 Conf., La Jolla, CA, US, March 24 - 28, 2003, (paper MOMT005) eConf C0303241 (2003), [arXiv:hep-ph/0306267].
- [20] A. Ferrari *et al.*, CERN Yellow Report 2005-10, INFN/TC\_05/11, SLAC-R-773 (2005).
- [21] F. Ballarini *et al.*, *Adv. Space Res.* **40** (2007) 1339.
- [22] M.V. Garzelli, Proc. ND2007, Int. Conf. on Nuclear Data for Science and Technology, April 22 - 27 2007, Nice, France, (editors O. Bersillon, F. Gunsing, E. Bauge, R. Jacqmin and S. Leray, EDP Sciences) (2008), 1129 [arXiv:0704.3917 [nucl-th]].
- [23] M.B. Tsang *et al.*, *Phys. Rev. Lett.* **86** (2001) 5023 [arXiv:nucl-ex/0103010].
- [24] A. Ono *et al.*, *Phys. Rev. C* **68** (2003) 051601 [arXiv:nucl-th/0305038].
- [25] D.V. Shetty *et al.*, *Phys. Rev. C* **76** (2007) 024606 [arXiv:0704.0471 [nucl-ex]].
- [26] D.V. Shetty *et al.*, *Phys. Rev. C* **71** (2005) 024602.
- [27] S. Wuenschel *et al.*, *Phys. Rev. C* **79** (2009) 061602.
- [28] L. Manduci *et al.*, *Nucl. Phys. A* **811** (2008) 93 [arXiv:0805.0975 [nucl-ex]].
- [29] M. Pichon *et al.*, *Nucl. Phys. A* **779** (2006) 267 [arXiv:nucl-ex/0602003].
- [30] K. Zhao *et al.*, *Phys. Rev. C* **79** (2009) 024614 [arXiv:0902.2631 [nucl-th]].